Resource Allocation Policies for Hybrid Power-Grid and Harvested Energy Communication Systems

Iman Valiulahi, Christos Masouros, *Senior Member*, IEEE

***Abstract*—This work studies resource allocation policies for a multi-antenna access point that is powered by a combination of harvested energy and the power grid, communicating with multiple single-antenna users. Traditionally, a single-antenna access point or orthogonal transmission was used for the throughput maximization problem. However, these methods are known to waste resources. To overcome this issue, we propose a non-convex problem to directly solve throughput maximization problem. Though the problem is changeling to solve, we first propose an iterative algorithm based on the first-order Taylor expansion and block coordinate descent for the scenario where full channel state information (CSI) and energy arrival information (EAI) are assumed to be known. Then, inspired by this scenario, we study a case in which statistical CSI and EAI are only required. Simulation results demonstrate that the energy-performance trade-off as well as the performance of the statistical case is comparable to the full CSI and EAI scenario, which supports the practically aspect of the proposed policies.**

***Index Terms*—Energy harvesting, resource allocation, first-order Taylor expansion, block coordinate descent.**

I. Introduction

Recently, there has been a growing interest in using energy harvesting (EH) sources for telecommunication tasks, where the access point is typically equipped with the EH tools to harvest energy from ambient energy sources such as solar, wind, and thermoelectric [1]. However, these energy sources are varied over time, resulting in the harvested energy changes with time. Thus, the literature is abundant in the dynamic resource allocation strategies for such a problem.

In [2], [3], and [4], the authors studied the EH multiple access, broadcast, and relay channels, respectively. To minimize the transmission time, in [5], the authors proposed optimal power allocation policies for an EH access point with an infinite battery capacity. This work was extended for the case where the capacity of the battery is finite in [6]. To obtain the best performance of any feasible resource allocation policies, in [7], for the single-user case, the authors studied the scenario where full channel state information (CSI) and energy arrival information (EAI) are known prior to the transmission begins. Joint power scheduling and antenna selection using zero-forcing (ZF) technique for the multi-antenna EH systems in the presence of the smart grid was studied in [8] in order to provide communication services for the multi-user scenario.

The previous works in the literature mainly focused on the simple scenarios such as point-to-point communication, the single-antenna access point, or orthogonal data transmission. These assumptions, however, are known to substantially waste resources. Accordingly, this paper studies a multiple-antenna EH communication system, communicating with multiple users in the presence of the power grid. More precisely, the required energy at the access point can be provided by both the EH and grid sources. We consider a battery with a finite capacity to store the energy whenever it is needed. We propose a non-convex problem to maximize the average system throughput constraint on the energy constraints–casualty, battery overflow, and the power grid–, quality of service (QoS) requested by all the users. The proposed problem can strike a balance between the consumed energy from both the sources and the communication performance. Though this problem is challenging to solve as it is not convex, we approximate the non-convex functions using the first-order Taylor expansion. Then, using the block coordinate descent, we provide an iterative algorithm to tighten the solution. We first obtain a performance benchmark using the full CSI and EAI. Then, we study the scenario where only requires the statistical CSI and EAI, which can be exploited in practice. The numerical results show an energy-performance trade-off as well as the performance obtained by the proposed polices is comparable to the energy-agnostic transmission.

II. System Model and Problem Formulation

As shown in Fig. 1, we consider a multi-antenna access point with N_t antennas equipped with an EH device and battery in the presence of the power grid, communicating with M single-antenna users. Following [6], the maximum capacity of the battery is considered as $E_{\max}$. Suppose that the total transmission time is $[0, T)$ and the energy arrives T_e times over this interval, following a Poisson process with rate λ_e. Also, the energy values, $e[i]$ for $i \in \{1, \cdots, T_e\}$, follow a uniform distribution with parameters $e_{\min}[i]$ and

The authors are with the Department of Electronic and Electrical Engineering, University College London, London WC1E 7JE, U.K. (e-mails: i.valiulahi@ucl.ac.uk; c.masouros@ucl.ac.uk)

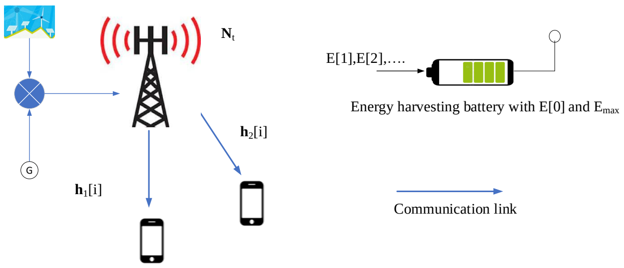

Fig. 1: System model.

$e_{\max}[i]$, i.e., $e[i] \backsim U(e_{\min}[i], e_{\max}[i])$ for $i \in \{1, \cdots, T_e\}$. We assume that the stored energy in the battery at the beginning of the transmission time, $t[0]$, is $e[0]$. In this paper, similar to [9], [10], we consider a full-duplex battery such that it can be charged or discharged at the same time. For the communication model, we assume a block fading channel where the channel states independently change T_c times, following a Poisson process with rate λ_c over the transmission time and remain constant during each block. Let us assume that all the users and antennas have the same coherence time though our model can be easily generalized for the case where each user and antenna has a different coherence time at the price of more parameters. The channel state vector between the access point and the m-th user at the i-th time slot is given by $\boldsymbol{h}_m[i] \in \mathbb{C}^{N_t \times 1}$. We define any change in the channel or energy as an event and the time interval between two consecutive events as the time slot. Thus, the number of events during the transmission time is $T_E = T_e + T_c$. As a result, the time slots can be written as $\ell[i] = t[i] - t[i-1], \ \forall i \in \mathcal{K} = \{1, 2, \cdots, T_E + 1\}$. It is worth noting that the first time slot is corresponding to the beginning of the transmission and first event. Also, the last time slot is for the last event and the end of transmission.

As shown in Fig. 1, the required energy at the access point, transmission and signal processing, can be provided by both the EH and grid sources. In particular, the power required for the $m-$th user at the $i-$th time slot can be written in the form of the summation of two sources as

$$\|\boldsymbol{w}_m[i]\|_2^2 = \phi p_m^e[i] + p_m^g[i], \tag{1}$$

where $p_m^e[i]$ and $p_m^g[i]$ are the portion of the power provided by the EH and grid sources for the $m-$th user and the $i-$th time slot, respectively. Moreover, the parameter ϕ can make a balance in energy consumption from the EH and non-renewable sources and $\|\cdot\|_2$ is the ℓ_2 norm. More precisely, setting $0 < \phi < 1$ encourages the access point to consume energy from the EH source. The required power at the $i-$th time slot by the signal processing, including the frequency synthesizer, mixer, digital to analog converter, and transmit filter, is modeled as

$$p_s[i] = \phi p_s^e[i] + p_s^g[i], \tag{2}$$

where $p_s^e[i]$ and $p_s^g[i]$ are the portion of the power provided by the EH device and grid at the i-th time slot, respectively. There are two inherent constraints on the harvested energy. First, the energy arrivals must not be consumed before being harvested, which is known as the casualty energy constraint. The following linear equations for all the time slots can satisfy this [6]

$$\sum_{i=1}^{k} \left(\sum_{m=1}^{M} \frac{1}{\eta} p_m^e[i] + p_s^e[i] \right) \ell[i] \leq \sum_{i=1}^{k} E_{in}[i], \ k \in \mathcal{K}, \tag{3}$$

where η is the efficiency of the power amplifier, which we assumed that is the same for all the antennas. $E_{in}[1] = e[0]$ and if the i-th event is an energy arrival, $E_{in}[\cdot] = e[\cdot]$, otherwise, $E_{in}[\cdot] = 0$. The second constraint states that the available energy at the battery must be greater than or equal to $E_{\max}$ to avoid the battery overflow, which can be satisfied by the following equations [6]

$$\sum_{i=1}^{k} \left(\sum_{m=1}^{M} \frac{1}{\eta} p_m^e[i] + p_s^e[i] \right) \ell[i] \geq \sum_{i=1}^{k} E_{in}[i] - p_s^e[i]\ell[i] - E_{\max}, \ k \in \mathcal{K}, \tag{4}$$

Moreover, the maximum power that can be provided by the grid is limited in each time slot. Thus, any resource allocation polices must satisfy the following constraints [10]

$$\sum_{i=1}^{k} \left(\sum_{m=1}^{M} \frac{1}{\eta} p_m^g[i] + p_s^g[i] \right) \ell[i] \leq p_{mg} \sum_{i=1}^{k} \ell[i], \ \forall k \in \mathcal{K}, \tag{5}$$

where p_{mg} is the maximum power that can be drawn from the grid source.

Traditionally, the orthogonal approaches such as the ZF method was used for the multiple antenna scenario. However, this method is known to waste the energy and resources and is not efficient for the case where there is no full information regarding the channel and energy arrival. To over come these issues, in this paper, we exploit the successive optimization technique to directly solve the resource allocation problem for the multiple antenna scenario. To do so, let us first define the Signal-to-interference-plus-noise ratio (SINR) as $\gamma_m[i] = \frac{|\boldsymbol{h}_m[i]^H \boldsymbol{w}_m[i]|^2}{\sum_{j \neq m} |\boldsymbol{h}_m[i]^H \boldsymbol{w}_m[i]|^2 + \sigma^2}, \forall m, i$, where $\sigma^2 = N_0 B$ in which N_0 and B are the spectral density of additive white Gaussian noise (AWGN) and the bandwidth of the system, respectively. Moreover, the term $\sum_{j \neq m}^{M} |\boldsymbol{h}_m[i]^H \boldsymbol{w}_m[i]|^2$ is the co-channel interference term at the m-th user caused by other users at the i-th time slot. Accordingly, the system throughout at the i-th time slot can be given by $R_m[i] = B \log_2 \big(1 + \gamma_m[i]\big)$. Our goal is to maximize the average system throughput over the transmission time subject to the energy and minimum QoS requested by the users. To do so, we propose the following optimization as

$$\max_{\substack{\boldsymbol{w}_m[i],p^g_m[i]\\ p^e_s[i],p^g_s[i],p^e_m[i]}} \frac{1}{M(T_E+1)}\sum_{i=1}^{T_E+1}\sum_{m=1}^{M} R_m[i]$$

$$\text{s.t.}, (1), (2), (3), (4), \text{ and } (5),$$

$$R_m[i] \geq R^{\mathrm{q}}, \quad \forall\, m, i, \tag{6a}$$

$$p^e_s[i], \text{ and } p^g_s[i] \geq 0, \forall m, i. \tag{6b}$$

Constraint (6a) is for the minimum QoS requested by all the users over the transmission time in which R^q is the minimum data rate. Constraint (6b) guarantees all the optimization variables are non-negative. Though R^q is not an optimization variable, it can strike a balance between the system throughput and energy consumption. It is difficult to solve problem (6) since the objective value and constraint (6a) are non-convex since the beamforming vectors appear in both the numerator and denominator of the SINR fraction. However, in the next section, we propose a novel solution for the proposed problem when full CSI and EAI are available, based on the first-order Taylor expansion of $R_m[i]$ and the block coordinate descent technique. It is worth clarifying that the value of the full CSI and EAI. This regime can provide the performance benchmark for any feasible resource allocations since full CSI and EAI are assumed to be available in advance. Moreover, this scenario paves the way to design the statistical policy by providing insight into the optimal resource allocation policies.

III. Throughput Maximization with the Full CSI and EAI

As mentioned, problem (6) is not convex, hence there is no efficient approach to solve it. To address this concern, in this section, we propose a novel solution based on the first-order Taylor expansion and the block coordinate descent. To do this, let us first define $\boldsymbol{W}_m[i] = \boldsymbol{w}_m[i]\boldsymbol{w}^H_m[i], \boldsymbol{Q}_m[i] = \boldsymbol{h}_m[i]\boldsymbol{h}^H_m[i]$, then, we can write $\|\boldsymbol{w}_m[i]\|^2_2 = \mathrm{tr}(\boldsymbol{w}_m[i]\boldsymbol{w}^H_m[i]) = \mathrm{tr}(\boldsymbol{W}_m[i]), |\boldsymbol{h}^H_m[i]\boldsymbol{w}_m[i]|^2 = \mathrm{tr}(\boldsymbol{h}_m[i]^H\boldsymbol{w}_m[i]\boldsymbol{h}^H_m[i]\boldsymbol{w}_m[i]) = \mathrm{tr}(\boldsymbol{Q}_m[i]\boldsymbol{W}_m[i])$. Consequently, the optimization problem in (6) can be recast as

$$\max_{\substack{\boldsymbol{W}_m[i]\\ p^e_s[i],p^g_s[i],p^e_m[i]}} \frac{B}{M(T_E+1)}\sum_{i=1}^{T_E+1}\sum_{m=1}^{M}\log_2\left(1+\frac{\mathrm{tr}(\boldsymbol{Q}_m[i]\boldsymbol{W}_m[i])}{\sum_{j\neq m}\mathrm{tr}(\boldsymbol{Q}_m[i]\boldsymbol{W}_j[i])+\sigma^2}\right)$$

$$\text{s.t.}, (2), (3), (4), \text{ and } (5),$$

$$\mathrm{tr}(\boldsymbol{W}_m[i]) = \phi p^g_m[i] + p^g_m[i], \tag{7a}$$

$$\log_2\left(1+\frac{\mathrm{tr}(\boldsymbol{Q}_m[i]\boldsymbol{W}_m[i])}{\sum_{j\neq m}\mathrm{tr}(\boldsymbol{Q}_m[i]\boldsymbol{W}_j[i])+\sigma^2}\right) \geq R^{\mathrm{q}}, \tag{7b}$$

$$p^e_s[i], \text{ and } p^g_s[i] \geq 0, ,$$

$$\mathrm{rank}(\boldsymbol{W}_m[i]) = 1, \forall m, i, \tag{7c}$$

where the last constraint ensures that the solution is rank-one. The problem is intractable because of the non-convexity of the data rate and rank-one constraint. To overcome these issues, we used the successive convex optimization technique in the following. Note that for any given convex function, $f(\boldsymbol{t})$, at the local point $\tilde{\boldsymbol{t}}$, there is the following lower bound $f(\boldsymbol{t}) \geq f(\tilde{\boldsymbol{t}}) + \nabla_{\boldsymbol{t}} f(\tilde{\boldsymbol{t}})^T(\boldsymbol{t}-\tilde{\boldsymbol{t}})$, where $\nabla_{\boldsymbol{t}} f(\tilde{\boldsymbol{t}})$ is the gradient of $f(\boldsymbol{t})$ at the local point $\tilde{\boldsymbol{t}}$ [11]. To exploit this bound for our problem, let us first simplify $R_m[i]$ as $R_m[i] = \log_2\Big(\sum_{j=1}^{M}\mathrm{tr}(\boldsymbol{Q}_m[i]\boldsymbol{W}_j[i]) + \sigma^2\Big) - \log_2\Big(\sum_{j\neq m}^{M}\mathrm{tr}(\boldsymbol{Q}_m[i]\boldsymbol{W}_m[i]) + \sigma^2\Big)$, where is still non-convex since it is a difference of two convex functions. By using the Taylor bound, we can obtain a lower bound on the second term at the local point $\tilde{\boldsymbol{W}}_m[i]$ as $-\log_2\Big(\sum_{j\neq m}^{M}\mathrm{tr}(\boldsymbol{Q}_m[i]\tilde{\boldsymbol{W}}_m[i]) + \sigma^2\Big) - \sum_{j\neq m}^{M}\mathrm{tr}\left(\frac{(\boldsymbol{W}_m[i]-\tilde{\boldsymbol{W}}_j[i])}{(\sum_{r\neq m}\tilde{\boldsymbol{W}}_r[i]+\sigma^2)\ln 2}\right)$. By dropping the rank-one constraint, problem (6) can be recast as

$$\max_{\substack{\boldsymbol{W}_m[i],p^g_m[i]\\ p^e_s[i],p^g_s[i],p^e_m[i]}} \frac{1}{T_E+1}\sum_{i=1}^{T_E+1}\sum_{m=1}^{M}\log_2\left(\sum_{j=1}^{M}\mathrm{tr}(\boldsymbol{Q}_m[i]\boldsymbol{W}_j[i])+\sigma^2\right) - \log_2\left(\sum_{j\neq 1}^{M}\mathrm{tr}(\boldsymbol{Q}_m[i]\tilde{\boldsymbol{W}}_m[i])+\sigma^2\right) - \sum_{j\neq m}^{M}\mathrm{tr}\left(\frac{(\boldsymbol{W}_m[i]-\tilde{\boldsymbol{W}}_j[i])}{(\sum_{r\neq m}\tilde{\boldsymbol{W}}_r[i]+\sigma^2)\ln 2}\right).$$

$$\text{s.t.}, (7a), (2), (3), (4), \text{ and } (5),$$

$$\log_2\left(\sum_{j=1}^{M}\mathrm{tr}(\boldsymbol{Q}_m[i]\boldsymbol{W}_j[i])+\sigma^2\right) - \log_2\left(\sum_{j\neq m}^{M}\mathrm{tr}(\boldsymbol{Q}_m[i]\tilde{\boldsymbol{W}}_m[i])+\sigma^2\right) - \sum_{j\neq m}^{M}\mathrm{tr}\left(\frac{(\boldsymbol{W}_m[i]-\tilde{\boldsymbol{W}}_j[i])}{(\sum_{r\neq m}\tilde{\boldsymbol{W}}_r[i]+\sigma^2)\ln 2}\right) \geq R^q, \forall i, m, \tag{8a}$$

which is convex and can be efficiently solved using off-the-shelf convex solvers such as CVX [12]. It is worth mentioning that by the lower bound derived used in (8), the feasible set of problem (8) will be a subset of the feasible set of problem (6). Hence, the objective value of problem (8) is less than the objective value of (8). Regarding the fact that the solution of the above problem is a linear approximation of the optimal solution, we tighten its solution using the block coordinate descent technique. More precisely, we first initialize the optimization variables, then solve problem (8), and use the solutions for the next iterations. We run this

Algorithm 1: The block coordinate descent method for solving problem (8).

1: Initialize $p_s^e[i], p_s^g[i], p_m^e[i], \boldsymbol{W}_m[i], p_m^g[i]$, set t and $\epsilon \ll 1$ as the iteration step and error tolerance, respectively.
2: **Repeat**
3: For given $p_{s,t}^e[i], p_{s,t}^g[i], p_{m,t}^e[i], \boldsymbol{W}_{m,t}[i], p_{m,t}^g[i]$, solve problem (8) and store the optimal solutions in $p_{s,t+1}^e[i], p_{s,t+1}^g[i], p_{m,t+1}^e[i], \boldsymbol{W}_{m,t+1}[i], p_{m,t+1}^g[i]$ and set $t = t+1$.
5: **Until** $\frac{\|\text{obj}^t - \text{obj}^{t-1}\|_2}{\|\text{obj}^{t-1}\|_2} \leq \epsilon$
Result: The final solutions are $p_{s,t}^e[i], p_{s,t}^g[i], p_{m,t}^e[i], \boldsymbol{W}_{m,t}[i], p_{m,t}^g[i]$.

iteratively until the termination criteria, $\frac{\|\text{obj}^t - \text{obj}^{t-1}\|_2}{\|\text{obj}^{t-1}\|_2} \leq \epsilon$, is satisfied, where ϵ is the tolerance error, obj is the objective value of problem (8) and t is the iteration step of Algorithm 1. The steps of the above procedure is summarized in Algorithm 1. Following our recent work [13] and regarding the fact that the optimal solution of problem (8) is increasing in each step, one can prove that Algorithm 1 is convergent. Using numerical simulations in Section V, we show that the proposed Algorithm 1 converges quickly.

Since the rank-one constraint is removed from the optimization problem, the solution might not be rank-one matrices. To overcome this issue, one can use the Gaussian randomization technique proposed in [14] constructing candidate sets of beamforming vectors from the solution of the proposed problem in (8) which satisfies the optimization constraints.

IV. Throughput Maximization with the Statistical CSI and EAI

In this section, inspired by the full CSI and EAI, we study the case where only statistical CSI and EAI are available. Since obtaining full CSI and EAI are challenging in many practical scenarios, the access point is not typically aware of the future channel states and energy arrivals. Below, we exploit a robust optimization technique for our proposed statistical policy. More precisely, using statistical CSI and EAI, we first determine the average number of events and their length during the transmission interval. Based on the fact that the combination of two independent Poisson processes is a Poisson process, we can conclude that the distribution of the events is a Poisson process with rate $\lambda_E = \lambda_e + \lambda_c$. Consequently, the expected number of events is $\bar{T}_E = \lambda_E T$. Now, let us assume that there is inexact information regarding CSI as below

$$|\bar{\boldsymbol{h}}_m[i]| \leq |\boldsymbol{h}_m[i]| \leq |\hat{\boldsymbol{h}}_m[i]|, \ \forall i, m, \tag{9}$$

which can be available through a long-term measurement in practice such that $|\bar{\boldsymbol{h}}_m[i]|$ and $|\hat{\boldsymbol{h}}_m[i]|$ are the minimum and maximum of the absolute value of the channel state vector for the m-th user at the i-th time slot. Consequently, the minimum throughput is $\bar{R}_m[i] = B\log\Bigg(1 + \frac{|\bar{\boldsymbol{h}}_m[i]^H \boldsymbol{w}_m[i]|^2}{\sum_{j\neq m}|\hat{\boldsymbol{h}}_m[i]^H \boldsymbol{w}_m[i]|^2 + \sigma^2}\Bigg)$. By assuming that the access point is currently working at the i_0-th time slot, we can write the following optimization for the i_0-th at the local point $\tilde{\boldsymbol{W}}_m[i]$ and future time slots as

$$\max_{\substack{\boldsymbol{W}_m[i], p_m^g[i] \\ p_s^e[i], p_s^g[i], p_m^e[i]}} \frac{1}{\bar{T}_E + 1 - i_0} \sum_{i=i_0}^{\bar{T}_E+1} \sum_{m=1}^{M} \Bigg[\log_2\Bigg(\sum_{j=1}^{M} \text{tr}(\bar{\boldsymbol{Q}}_m[i]\boldsymbol{W}_j[i]) + \sigma^2\Bigg) - \log_2\Bigg(\sum_{j\neq m}^{M} \text{tr}(\hat{\boldsymbol{Q}}_m[i]\tilde{\boldsymbol{W}}_m[i]) + \sigma^2\Bigg) - \sum_{j\neq m}^{M} \text{tr}\Bigg(\frac{(\boldsymbol{W}_m[i] - \tilde{\boldsymbol{W}}_j[i])}{(\sum_{r\neq m}\tilde{\boldsymbol{W}}_r[i] + \sigma^2)\ln 2}\Bigg)\Bigg]$$
$$\text{s.t.}, (7a), (2), (3), (4), \text{ and } (5),$$

$$\log_2\Bigg(\sum_{j=1}^{M} \text{tr}(\bar{\boldsymbol{Q}}_m[i]\boldsymbol{W}_j[i]) + \sigma^2\Bigg) - \log_2\Bigg(\sum_{j\neq m}^{M} \text{tr}(\hat{\boldsymbol{Q}}_m[i]\tilde{\boldsymbol{W}}_m[i]) + \sigma^2\Bigg) - \sum_{j\neq m}^{M} \text{tr}\Bigg(\frac{(\boldsymbol{W}_m[i] - \tilde{\boldsymbol{W}}_j[i])}{(\sum_{r\neq m}\tilde{\boldsymbol{W}}_r[i] + \sigma^2)\ln 2}\Bigg) \geq \bar{R}^{\text{q}}, \quad \forall i \in \{i_{0,\cdots,\bar{T}_E+1}\}. \tag{10a}$$

Note that all the constraints must be adopted for the i_0-th time slot, $\bar{T}_E$, and minimum energy arrival, however, to avoid excessive clutter, we only show this for constraint (3) as

$$\sum_{i=1}^{k}\Bigg(\sum_{m=1}^{M}\frac{1}{\eta}p_m^e[i] + p_s^e[i]\Bigg)\ell[i] \leq \sum_{i=1}^{k}\bar{E}_{in}[i], \quad k \in \{i_0, \cdots, \bar{T}_E + 1\}, \tag{11}$$

where $\bar{E}_{in}[1] = e[0]$ and if the i-th event is an energy arrival, $E_{in}[\cdot] = e_{\min}[\cdot]$, otherwise, $E_{in}[\cdot] = 0$. Problem (6) is convex and can be efficiently solved using CVX. Then, the solution can be tightened using proposed Algorithm 1. In the simulation results, we compare the performance of the full and statistical CSI and EAI. The last but not the least is that the rank-one constraint is also necessary for the statistical problem, however, using the Gaussian randomization technique proposed in [14], one can obtain a rank-one solution for problem (10).

V. Experiments

This section provides Monte Carlo simulations to investigate the performance of the proposed resource allocation policies. The bandwidth and noise power spectral

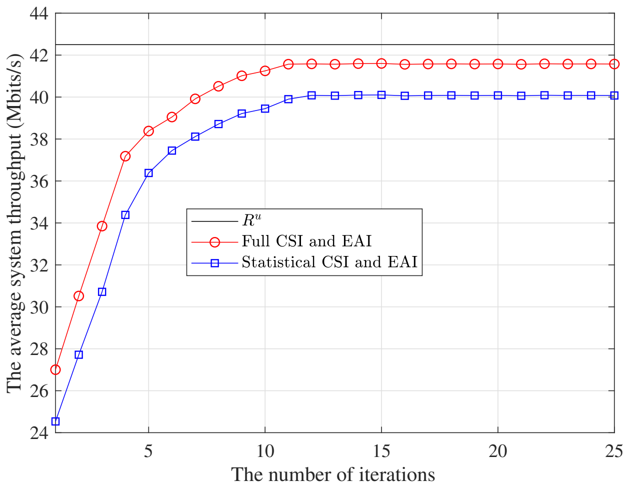

Fig. 2: The average system throughput versus the number of iterations, evaluating the convergence behavior of the proposed policies for $M = 4$ users, $\lambda_c = 1$ 1/s, $\lambda_e = 60$ J/sm, $p_{mg} = 30$ dBm, and $N_t = 10$.

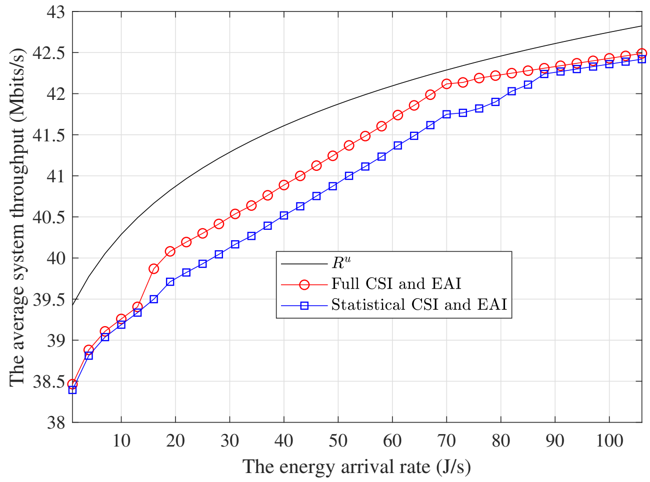

Fig. 3: The average system throughput versus the rate of energy arrivals for $M = 4$ users, $\lambda_c = 1$ 1/J, and $p_{mg} = 30$ dBm, $N_t = 10$.

density are assumed to be $B = 1$ mega Hertz (MHz) and $N_0 = 10^{-13}$ W/Hz, respectively. The Rayleigh channel model with complex normal variables with the mean and variance, $\mu_c = 5 \times 10^{-5}$ and $\sigma_c^2 = 10^{-10}$, are considered for the simulations for all the users. The tolerance error in Algorithm 1 is set to be $\epsilon = 10^{-4}$. The number of antennas $N_t = 10$. Moreover, we initialize the variables of Algorithm 1 randomly. To evaluate the performance better, an upper bound on the objective value of the proposed problem is derived as $R^{ub} = B \log_2 \left(1 + \frac{|\hat{\boldsymbol{h}}_m[i]|^2 p_{\max}}{N_0 B}\right)$, where $|\hat{\boldsymbol{h}}_m[i]|$ is the maximum of the absolute value of channel obtained by μ_c and σ_c. Also, the maximum power can be calculated by $p_{\max} = \frac{E^{\max} + p_{mg}}{\lambda_E}$ where $E^{\max} = e_{\max}[i]$ for all i. We set $p_s = 40$ dBm as the static circuit power consumption [10]. The minimum data rate is set to be $R^q = 5$ megabits per second (Mbits/s). The transmission interval is assumed to be 5 seconds, i.e., $(0, 5]$. The maximum capacity of the battery is set to be $E_{\max} = 500$ joule (J). Without loss of generality, we assume that $e_{min}[i] = 2$ J and $e_{\max}[i] = 5$ J. We set $\phi = 0.01$ to ensure that the access point prefers to consume energy from the EH source. The power amplifier's efficiency is set to be $\eta = 0.35$. The maximum power that can be drawn from the grid will be specified in each simulation. For a fair comparison, we set $i_0 = 1$ in problem (10). We exploit the full CSI an EAI scenario as the performance benchmark for the statistical case.

A. Converge Behavior of the Proposed Policies

We commence our evaluations by investigating the convergence behavior of the proposed policies in Fig. 2 for $M = 4$ users. For this simulation, we set $p_{mg} = 30$ dBm, $\lambda_c = 1$ 1/s, and $\lambda_e = 1$ J/s. It is observed from this figure that the proposed policies quickly converge after almost 12 iterations. The performance of the scenario where full CSI and EAI are assumed to be available at the access point serves as a benchmark for the statistical scenario. Moreover, this performance is comparable to the maximum achievable throughput, R^{ub}.

B. The Average System Throughput Versus the Energy Arrival Rate

In Fig. 3, we evaluate the average system throughput versus the different values of energy arrival rate for $M = 4$ users, $\lambda_c = 1$ 1/s, and $p_{mg} = 30$ dBm over 100 Monte Carlo simulations. Intuitively, by increasing the energy arrival rate, it is expected to achieve better performance in terms of the system throughput for all the methods as shown in Fig. 3. This is because of the fact that more energy is available at the access point. It is also observed from this figure that the performance of the statistical scenario is close to the benchmark (the full CSI ane EAI scenario) in both the low and high energy arrival rates. More precisely, when the energy arrival rate is low, the access point is mainly relied on the grid source for its operations. Thus, prior knowledge about the future energy arrivals has a low effect on the resource allocation policies, approaching the statistical scenario's performance to the the full CSI and EAI case. On the other hand, in case of high rate regime, the EH source will be a continuous energy source. Consequently, information regarding the energy arrivals in the future time slots is less valuable in the resource allocation policies because energy is always available at the access point.

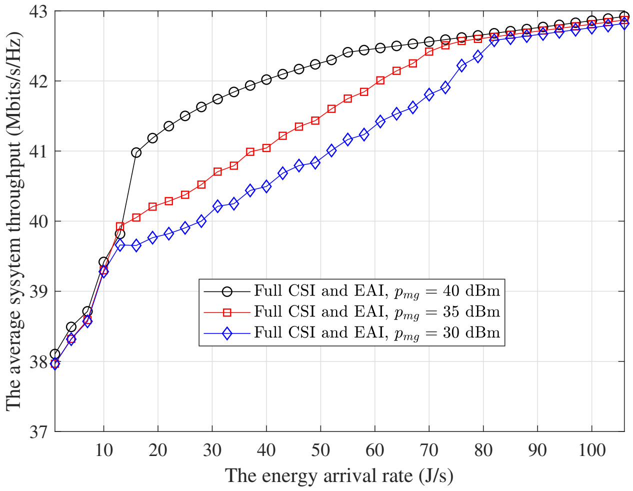

Fig. 4: The average system throughput versus the rate of energy arrivals for the different values of p_{mg}, $M = 4$ users, $\lambda_c = 1$ 1/J.

In Fig. 4, we depict the average system throughput versus the rate of energy arrivals for the different values of P_{mg} in order to evaluate the effect of the maximum energy that can be drawn from the grid on the proposed policies. To avoid excessive clutters, we only consider the full CSI and EAI scenario. From this figure, one can understand that a higher value of p_{mg} results in better performance in terms of the throughput. This is mainly because of the fact that with a large value of p_{mg}, the grid can provide energy for the access point operation whenever energy at the battery is low, enhancing the throughput. In Addition, it is observed that the performance slightly diminishes when the energy arrival rate is high. This comes from the fact that the access point prefers to consume the energy from the EH source, which means that for the high value of energy arrival rate, the access point relies on the EH source and p_{mg} is less important for the resource allocation policies, approaching the results for all the different values of p_{mg}.

VI. Conclusion

This paper studied the full and statistical CSI and EAI policies for a multi-antenna EH communication system in the presence of the power grid, serving multiple users. We proposed a non-convex optimization in order to maximize the average system throughput subject to the energy and QoS constraints. Using the first-Taylor expansion and block coordinate descent techniques, we solved the proposed problem for the full CSI ane EAI regime. Then, motivated by this policy, we developed the statistical policy. Simulation evaluations were done to investigate the performance of the proposed approaches and showed that it is comparable to the energy-agnostic transmission approach.

Acknowledgment

This project has received funding from the European Union's Horizon 2020 research and innovation program under the Marie Skłodowska-Curie grant agreement No 812991.

References

[1] C. Park and P. H. Chou, "Ambimax: Autonomous energy harvesting platform for multi-supply wireless sensor nodes," in *2006 3rd annual IEEE communications society on sensor and ad hoc communications and networks*, vol. 1, pp. 168–177, IEEE, 2006.

[2] J. Yang and S. Ulukus, "Optimal packet scheduling in a multiple access channel with energy harvesting transmitters," *Journal of Communications and Networks*, vol. 14, no. 2, pp. 140–150, 2012.

[3] A. A. Nasir, X. Zhou, S. Durrani, and R. A. Kennedy, "Relaying protocols for wireless energy harvesting and information processing," *IEEE Transactions on Wireless Communications*, vol. 12, no. 7, pp. 3622–3636, 2013.

[4] J. Yang, O. Ozel, and S. Ulukus, "Broadcasting with an energy harvesting rechargeable transmitter," *IEEE Transactions on Wireless Communications*, vol. 11, no. 2, pp. 571–583, 2011.

[5] J. Yang and S. Ulukus, "Optimal packet scheduling in an energy harvesting communication system," *IEEE Transactions on Communications*, vol. 60, no. 1, pp. 220–230, 2011.

[6] K. Tutuncuoglu and A. Yener, "Optimum transmission policies for battery limited energy harvesting nodes," *IEEE Transactions on Wireless Communications*, vol. 11, no. 3, pp. 1180–1189, 2012.

[7] O. Ozel, K. Tutuncuoglu, J. Yang, S. Ulukus, and A. Yener, "Transmission with energy harvesting nodes in fading wireless channels: Optimal policies," *IEEE Journal on Selected Areas in Communications*, vol. 29, no. 8, pp. 1732–1743, 2011.

[8] Z. Zhou, H. Yu, S. Mumtaz, S. Al-Rubaye, A. Tsourdos, and R. Q. Hu, "Power control optimization for large-scale multi-antenna systems," *IEEE Transactions on Wireless Communications*, vol. 19, no. 11, pp. 7339–7352, 2020.

[9] O. Orhan, D. Gündüz, and E. Erkip, "Energy harvesting broadband communication systems with processing energy cost," *IEEE Transactions on Wireless Communications*, vol. 13, no. 11, pp. 6095–6107, 2014.

[10] D. W. K. Ng, E. S. Lo, and R. Schober, "Energy-efficient resource allocation in ofdma systems with hybrid energy harvesting base station," *IEEE Transactions on Wireless Communications*, vol. 12, no. 7, pp. 3412–3427, 2013.

[11] S. Boyd and L. Vandenberghe, *Convex optimization*. Cambridge university press, 2004.

[12] M. Grant, S. Boyd, and Y. Ye, "Cvx: Matlab software for disciplined convex programming," 2008.

[13] I. Valiulahi and C. Masouros, "Multi-uav deployment for throughput maximization in the presence of co-channel interference," *IEEE Internet of Things Journal*, 2020.

[14] E. Karipidis, N. D. Sidiropoulos, and Z.-Q. Luo, "Quality of service and max-min fair transmit beamforming to multiple cochannel multicast groups," *IEEE Transactions on Signal Processing*, vol. 56, no. 3, pp. 1268–1279, 2008.